Leveraging Hybrid UAV Relays in Adverse Weather for FSO Link Capacity Maximization

Muhammad Nafees, Shenjie Huang, John Thompson, Majid Safari
School of Engineering, Institute for Digital Communications, The University of Edinburgh, Edinburgh, EH9 3JL, UK
Email: {m.nafees, shenjie.huang, john.thompson, majid.safari}@ed.ac.uk

2022 IEEE Wireless Communications and Networking Conference (WCNC) | 978-1-6654-4266-4/22/$31.00 ©2022 IEEE | DOI: 10.1109/WCNC51071.2022.9771966

***Abstract*—In the context of beyond the fifth-generation (B5G), free-space optics (FSO) is a vital technology for high data rate applications because of its low cost and licence-free high bandwidth. However, during adverse weather, the FSO link's capacity can be significantly impacted, and establishing parallel radio frequency (RF) backup links just for occasional utilization is both complex and costly. In this study, in order to improve the availability of FSO link in adverse weather conditions, we propose to use unmanned aerial vehicles (UAVs) as hybrid relays to intercept an FSO link. The UAVs construct an intermediate millimeter wave (MMW) link, while ensuring that the approach has no impact on the source and destination. The end-to-end system capacity is maximized by optimizing UAVs' location based on the negatively correlated FSO and MMW link length. The performance of the proposed model is compared to benchmark systems such as single FSO, fixed relay-assisted FSO, and fixed hybrid FSO/RF systems. The numerical results clearly demonstrate the proposed scheme's superiority. Finally, using weather statistics from the cities of Edinburgh and London in the United Kingdom, the performance of the proposed system and its counterparts in realistic scenarios is demonstrated, which illustrates that the proposed system may significantly improve link availability towards the carrier-class criterion.**

***Index Terms*—Beyond fifth-generation (B5G), unmanned aerial vehicles (UAVs), free-space optics (FSO), millimeter wave (MMW) .**

I. Introduction

Beyond the fifth-generation (B5G) wireless networks are expected to improve data speeds and quality-of-service (QoS) by addressing existing network limitations. Free-space optical (FSO) communication is predicted to be critical for backhauling in B5G [1]. Because of their ease of deployment, quick setup time, and cheap maintenance costs, FSO links are a possible alternative to traditional fiber optics used for backhaul connectivity. However, FSO links suffer from atmospheric loss owing to fog and scintillation. In light and moderate fog, increasing transmit power can help, but in thick and deep fog, power control has a very negligible impact due to the significant path loss [2]. Radio frequency (RF) link is an excellent complement to FSO because it is insensitive to fog and could easily penetrate it. Millimeter wave (MMW) systems, which operate between 30 and 300 GHz, have two attractive properties as a potential candidate for hybrid networks in B5G. There is an order-of-magnitude greater available bandwidth in MMW bands than in microwave, which is one of the key advantages. Secondly, because MMW has a short wavelength, antennas may be shrunk and tightly integrated into compact dimensions.

To combine the benefits of both links, some hybrid paradigms including both RF and FSO links have been developed for high data rate backhauling. In the case of parallel links, there are two categories of hybrid FSO/RF systems: switch-over [3] and simultaneous transmission [4]. Serial fixed multi-hop relaying e.g., hybrid [5] or FSO-only [6] are other benchmark schemes. Despite the fact that FSO normally works effectively, these solutions require permanent RF installations. Besides added complexity, fixed FSO-only relaying can be compromised by fog.

Unmanned aerial vehicles (UAVs), with their 3D mobility and autonomous flying capabilities, will be increasingly utilized in future wireless networks [7]. Several studies (e.g., [8], [9]) have shown that UAV-to-Everything (U2X) links can be successfully established using FSO beams. In [10], the performance of a UAV-assisted backhauling architecture in a realistic 3D model of Ghent, Belgium, is studied. UAV-aided air-to-air communication is used in [9] to provide excellent line-of-sight (LOS) connectivity for the FSO system. A hybrid FSO/RF communication technique is also used for the air-to-ground link, with RF functioning as a backup for FSO in adverse weather.

Owing to the increasing demand for FSO links, it is reasonable to assume that all FSO links cannot have parallel RF transmission links. Because FSO links perform better under more frequent favourable weather situations, it is both complex and costly to build RF links which are usually dormant. In terms of an efficient solution, the co-authors [11] proposed a game-theoretic scheme to use spectrum from nearby RF nodes to send data when a backhaul FSO link is compromised by rare fog events. Motivated by the growing demand for UAV deployment as relays, we propose a novel method for enhancing the end-to-end capacity of a fog-troubled FSO link. The hybrid UAV relays intercept the FSO link to create an intermediate MMW link; the FSO signal attenuation level determines the optimal placement of UAVs, which defines the coverage of FSO and MMW links to maximize the end-to-end capacity. As the fog event passes, the UAVs may be withdrawn and the FSO link can resume regular operation without relays.

This paper is organized as follows. In Section II, we introduce the proposed model and describe the FSO and MMW channel models. Section III covers the benchmark systems and provides a method for optimizing the deployment of UAVs for the proposed model. The numerical results are presented and discussed in section IV. In Section V, we evaluate and

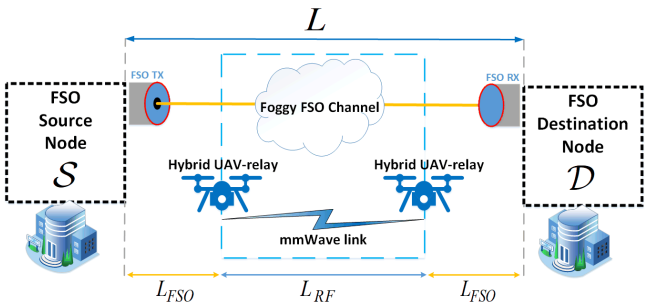

Fig. 1. The proposed system model.

discuss the performance of all the models based on practical measurements. The paper is concluded in section VI.

II. System Model

Consider the system model presented in Fig. 1. Specifically, two hybrid FSO/RF UAV relays intercept the FSO link during adverse weather. The first relay converts the received optical signal to RF before retransmission, while the second relay converts the received RF signal back to an optical signal. As a result, the FSO source and destination require no additional functionality or backup RF links. The decode-and-forward (DF) multi-hop transmission system attains higher capacity than the corresponding amplify-and-forward (AF) multi-hop transmission system [12]. To this end, it is presumed that all the UAV-assisted and fixed relays are capable of DF relaying. The precise pointing, acquisition, and tracking (PAT) method is assumed to be able to compensate for the pointing errors [13]. Also, it is assumed that all FSO transceivers have the same specifications. Furthermore, UAVs can operate with on-board batteries for several hours and tethered UAVs can be employed for longer flying periods at low altitudes.

A. Channel Model

1) FSO Channel Model: When intensity modulation direct detection (IM/DD) is used in the FSO link, the received electrical signal may be expressed as

$$s_1 = \rho g_1 h_1 x_1 + z_1, \tag{1}$$

where ρ denotes the responsivity of the photo-detector, g_1 is the average gain to the receiver optical power, x_1 refers to the transmitted optical intensity, s_1 represents the received electrical signal and the zero-mean real Gaussian noise with variance σ_1^2 is denoted by z_1. There is an inverse correlation between atmospheric turbulence and fog [14], hence the turbulence-induced intensity fading h_1 is ignored in this paper. The average gain g_1 can be expressed as [15]

$$g_1 = \frac{A}{\pi\left(\frac{\phi}{2}L_{FSO}\right)^2}\exp^{-(\kappa L_{FSO})}, \tag{2}$$

where $A = \pi\left(\frac{d}{2}\right)^2$, the first and second terms represent geometric and weather-related atmospheric losses owing to scattering and absorption, respectively. The diameter of the receiver aperture is denoted by d, ϕ represents the beam divergence angle, L_{FSO} shows the link distance from FSO source to the destination, and κ is a weather-dependent attenuation coefficient determined based on the Beer-Lambert law. The attenuation coefficient κ and the visibility V in km are related as $\kappa = \frac{3.91}{V}\left(\frac{\lambda_1}{550\times10^{-9}}\right)^{-\xi}$, where λ_1 is the optical wavelength and ξ is the weather condition based size distribution of the scattering particles. It is defined as a function of visibility distance as [16]

$$\xi = \begin{cases} 1.6, & V > 50\,\text{km} \\ 1.3, & 6\,\text{km} < V < 50\,\text{km} \\ 0.16V + 0.34, & 1\,\text{km} < V < 6\,\text{km} \\ V - 0.5, & 0.5\,\text{km} < V < 1\,\text{km} \\ 0, & V < 0.5\,\text{km} \end{cases}. \tag{3}$$

Based on (1), the achievable rate (channel capacity lower bound) of an IM/DD FSO link is given by [11]

$$C^{\text{FSO}} = \frac{1}{2}W_1\log_2\left(1 + \frac{eP_1^2 g_1^2 \rho^2}{2\pi\sigma_1^2}\right), \tag{4}$$

where W_1 denotes the bandwidth of the FSO link, e is the base of natural logarithm and P_1 represent the optical transmission power. Substituting (2) into (4), we have

$$C^{FSO} = \frac{W_1}{2}\log_2\left(1 + \frac{e\rho^2 d^4 P_1^2 \exp^{-(2\kappa L_{FSO})}}{2\pi\sigma_1^2\phi^4 L_{FSO}^4}\right), \tag{5}$$

consider $\Omega_1 = \frac{e\rho^2 d^4 P_1^2}{2\pi\sigma_1^2\phi^4}$ represents the constant terms, then (5) can be simplified as

$$C^{FSO} = \frac{W_1}{2}\log_2\left(1 + \frac{\Omega_1\exp^{-(2\kappa L_{FSO})}}{L_{FSO}^4}\right). \tag{6}$$

2) RF Channel Model: The RF channel may be stated as

$$s_2 = \sqrt{P_2}\sqrt{g_2}h_2 x_2 + n_2, \tag{7}$$

where P_2, g_2, h_2 denote transmit power, average power gain, and the fading gain, respectively, s_2 and x_2 are the received and transmitted signal, respectively, and n_2 refers to the zero-mean complex Gaussian noise with power spectral density N_o. Since measurements [17] reveal that small-scale fading has negligible impact on received power in MMW systems using highly directional antennas, the fading gain h_2 is neglected in this work. Using a carrier frequency f_c = 60 GHz, the effective gain can be stated as [18]

$$g_2[dB] = G_t + G_r - 20\log_{10}\left(\frac{4\pi L_{RF}}{\lambda_2}\right) - L_{RF}(\alpha_{oxy} + \alpha_r), \tag{8}$$

where G_t and G_r are the transmit and receive antenna gains, λ_2 is the RF wavelength at f_c, α_{oxy} and α_r are the attenuation induced by oxygen absorption and rain, respectively. As only foggy conditions are considered, the impact of α_r on MMW transmission can be disregarded from (8). Fog can severely impact the FSO transmission, but fog-based attenuation is negligible for RF below 100 GHz frequencies [19], hence its

effect on 60 GHz MMW transmission is neglected. Based on (7), the achievable rate over the MMW link is given by [20]

$$C^{\mathrm{RF}} = W_2 \log_2 \left(1 + \frac{P_2 g_2}{\sigma_2^2}\right), \tag{9}$$

where W_2 is the RF bandwidth and σ_2^2 is the RF noise variance. Substituting g_2 from (8) into (9), we get

$$C^{\mathrm{RF}} = W_2 \log_2 \left(1 + \frac{P_2 G_t G_r}{\sigma_2^2 \left(\frac{4\pi L_{RF}}{\lambda_2}\right)^2 \left(\frac{L_{RF} 10^{\alpha_{oxy}/10}}{1000}\right)}\right), \tag{10}$$

using $\Omega_2 = \frac{1000 P_2 G_t G_r \lambda_2^2}{16\pi^2 \sigma_2^2 10^{\alpha_{oxy}/10}}$ which represents all the constant terms, we can simplify (10) as

$$C^{\mathrm{RF}} = W_2 \log_2 \left(1 + \frac{\Omega_2}{L_{RF}^3}\right). \tag{11}$$

III. FSO/RF Relaying Systems

The benchmark relay-assisted FSO and hybrid FSO/RF relaying systems are briefly described in this section, followed by further details on our proposed model. Fig. 2 depicts all the models used in this paper along with conventional single FSO link case in Fig. 2(a). In addition to the single FSO link, one can note that two benchmark three-hop systems are considered for a consistent comparison with the proposed model.

A. Fixed Multi-hop FSO Relaying System

In this system, we investigate a three-hop FSO system as shown in Fig. 2(b) with two relays $\mathcal{R}_1$ and $\mathcal{R}_2$ positioned at equal distances $\frac{L}{3}$ and $\frac{2L}{3}$ between $\mathcal{S}$ and $\mathcal{D}$, respectively. This is referred to as **f**ixed-**o**ptical **r**elaying (FOR) in this paper.

B. Fixed Hybrid FSO/RF Relaying

We consider a fixed three-hop hybrid FSO/RF relaying system with an MMW link in the middle and FSO links in the first and third hops, as illustrated in Fig. 2(c). The first hybrid relay $\mathcal{R}_1$ converts the received optical signal to RF (optical-RF down conversion) and the second relay $\mathcal{R}_2$ converts the RF signal back into an optical signal (RF-optical up conversion) before retransmission to the destination $\mathcal{D}$. This model is named as **f**ixed-**h**ybrid **r**elaying (FHR) in this work.

C. Hybrid UAV-assisted Relaying

The proposed model, shown in Fig. 2(d), is referred to as **h**ybrid **U**AV-assisted **r**elaying (HUR). It is essentially a flexible form of FHR in which we use the mobility of UAVs to respond to weather attenuation in order to get the most out of both FSO and MMW links. Considering DF relaying is employed, the end-to-end capacity $C_{\mathcal{SD}}$ for proposed HUR and the FHR schemes can be stated as

$$C_{\mathcal{SD}} = \min\left(C_1^{FSO}, C^{RF}, C_2^{FSO}\right), \tag{12}$$

where ${C_1}^{FSO}$, C^{RF} and ${C_2}^{FSO}$ are the achievable rates of the links $\mathcal{S}-\mathcal{R}_1$, $\mathcal{R}_1-\mathcal{R}_2$ and $\mathcal{R}_2-\mathcal{D}$, respectively. Making use of the symmetric FSO links and similar FSO transceivers, (12) can be further reduced as $C_{\mathcal{SD}} = \min\left(C^{FSO}, C^{RF}\right)$,

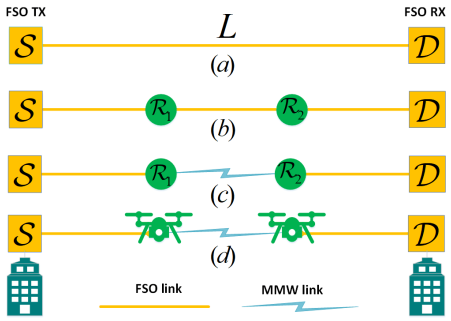

Fig. 2. The (a) single FSO link (b) fixed-optical relaying (c) fixed-hybrid relaying (d) hybrid UAV-assisted relaying.

where C^{FSO} represents both ${C_1}^{FSO}$ and ${C_2}^{FSO}$. Assuming identical system parameters when FOR system is used, any single hop's capacity is also its $C_{\mathcal{SD}}$. In the proposed system, the positions of UAV relays determine the length of FSO and MMW links. Note that L_{FSO} and L_{RF} denote the link coverage distance for FSO (e.g., both hops have equal link distance L_{FSO}) and MMW links, respectively. We make use of the positions of stationary relays $\mathcal{R}_1$ and $\mathcal{R}_2$ at distance $\frac{L}{3}$ and $\frac{2L}{3}$ from the source $\mathcal{S}$, respectively, as a reference point for the UAV relays. Assigning a variable χ to evaluate the negative correlation between the coverage distance of FSO and MMW links in the proposed model as

$$L_{FSO} = \frac{L - 3\chi}{3} \tag{13}$$

and

$$L_{RF} = \frac{L + 6\chi}{3}. \tag{14}$$

It's worth noting that a serial relaying system's capacity is optimal when the individual links' capacities are comparable or ideally equal (and non-zero) for a given set of system parameters. To this end, the optimal solution can be obtained by positioning UAVs to determine the optimal link coverage for both FSO and MMW links that maximizes the system's capacity during the fog event. Consequently, we substitute (13) and (14) into (6) and (11), respectively, and compare both as

$$\frac{W_1}{2}\log_2 \left(1 + \frac{\Omega_1 \exp^{-(2\kappa L_{FSO})}}{L_{FSO}^4}\right) = W_2 \log_2 \left(1 + \frac{\Omega_2}{L_{RF}^3}\right), \tag{15}$$

by using properties of logarithms, we can write (15) as

$$\left(1 + \frac{\Omega_1 \exp^{-(2\kappa L_{FSO})}}{L_{FSO}^4}\right)^{\frac{W_1}{2W_2}} = \left(1 + \frac{\Omega_2}{L_{RF}^3}\right), \tag{16}$$

then from (13) and (14) we can write

$$\left(1 + \frac{81\Omega_1 \exp^{-\frac{2\kappa}{3}(L-3\chi)}}{(L-3\chi)^4}\right)^{\frac{W_1}{2W_2}} = \left(1 + \frac{27\Omega_2}{(L+3\chi)^3}\right). \tag{17}$$

One can see that (17) is nonlinear equation which cannot be solved for χ using standard methods. We exploit the Newton-Raphson (NR) method which is the most popular among numerical methods due to its speed of convergence and ease

of implementation [21]. By iterating the scheme, NR aims at finding the root of a function $f(\chi)$. Let

$$f(\chi) = \left(1 + \frac{81\Omega_1 \exp^{-\frac{2\kappa}{3}(L-3\chi)}}{(L-3\chi)^4}\right)^{\frac{W_1}{2W_2}} - \left(1 + \frac{27\Omega_2}{(L+3\chi)^3}\right), \tag{18}$$

Algorithm 1: Optimal FSO and MMW Link Coverage

Input : All system parameters (i.e., W_1, W_2, κ, etc.)
Output: Optimal χ and subsequent UAVs positions
initialize;
$\chi[1] \in [\chi_{min}, \chi_{max}]$,
for $i = 1 : \mathcal{N}_{max}$ **do**
  Evaluate the $f(\chi[i])$ from (17)
  Compute $\frac{\partial f(\chi[i])}{\partial \chi}$ from (19)
  Update the NR expression:
  $\chi[i+1] = \chi[i] - \frac{f(\chi[i])}{\frac{\partial}{\partial \chi} f(\chi[i])}$
end
return χ as optimal value that maximizes $C_{\mathcal{SD}}$

then the first derivative of (18) w.r.t χ is computed in (19). The NR method quickly converges, however this convergence might be compromised if the initial value (i.e., $\chi[1]$) is out of the practical limits. To tackle this, we can set a minimum link length for both FSO and MMW links denoted by L_{FSO}^{min} and L_{RF}^{min}, respectively. Then, χ_{max} and χ_{min} can be obtain by substituting L_{FSO}^{min} and L_{RF}^{min} into (13) and (14), respectively. Consequently, the initial value of $\chi \in [\chi_{min}, \chi_{max}]$. The steps to find the optimal χ for (17) are summarized in Algorithm 1. The deployment positions of both UAVs are easily determined once an optimal value of χ is obtained.

IV. Results and System Performance

This section presents some simulation results for our proposed wireless backhauling system depicted in Fig. 1. The system parameters used in the numerical simulations are listed in Table I. The total link distance $L = 1000$ m, unless stated otherwise. For the benchmark single FSO link scheme, the link distance $L_{FSO} = L$. The attenuation in dB/km is related to the weather-dependent attenuation coefficient by 4.343κ [22]. The RF noise variance $\sigma_2^2[dB] = W_2 N_o + N_f$ where W_2, N_o, and N_f denote the MMW bandwidth, power spectral density of noise (dBm/MHz), and receiver noise figure, respectively [20]. For simplicity the transmit power for both FSO and MMW links is assumed to be equal i.e., $P_1 = P_2$. Also, both L_{FSO}^{min} and L_{RF}^{min} are assumed to be 10 m.

Fig. 3 illustrates the end-to-end capacity of the proposed HUR, state-of-the-art single FSO, and fixed relay-assisted FOR and FHR systems. When the fog-based attenuation $\kappa <$ 18 dB/km, the proposed HUR method is initially outperformed by the FOR model. This is due to the fact that visibility is still adequate for the three-hop FSO links, and the system benefits from FSO relays' high performance at low weather attenuation. However, as the weather attenuation increases, the proposed HUR scheme outperforms all three alternative deployments by a growing margin. It is also worth noting that at about $\kappa \geq 18$ dB/km, both FOR and FHR systems perform identically thereon, because capacity is limited in both cases by FSO hops due to an increased weather attenuation.

TABLE I. Simulation Parameters

FSO Link [11]		
Parameter	Symbol	Value
FSO wavelength	λ_1	1550 nm
Receiver diameter	d	5 cm
Beam divergence angle	ϕ	3.5 mrad
Responsivity	ρ	0.5 V^{-1}
Noise variance	σ_1^2	$10^{-14}A^2$
Transmit power	P_1	20 dBm
Bandwidth	W_1	1 GHz
Link distance	L	1000 m
MMW RF Link [18]		
Parameter	Symbol	Value
Carrier Frequency	f_c	60 GHz
Bandwidth	W_2	800 MHz
Transmit power	P_2	20 dBm
Transmitter gain	G_t	44 dBi
Receiver gain	G_r	44 dBi
Oxygen absorption	α_{oxy}	15.1 dB/km
Receiver noise figure	N_f	5 dB
Noise power density	N_o	-114 dBm/MHz

Fig. 4 shows that as the weather deteriorates, the FSO links surrender more link coverage to the MMW link between $\mathcal{S}$ and $\mathcal{D}$. That is, both UAV relays move closer to the source and destination FSO nodes. For example, at κ = 48 dB/km, the FSO link shrinks to about 250 m i.e., both FSO hops cover 500 m and the remaining half is covered by a single MMW link to optimize the $C_{\mathcal{SD}}$. In Fig. 5, we illustrate the performance of all the deployments for various distances L from $\mathcal{S}$ to $\mathcal{D}$ during low visibility. The proposed HUR system clearly performs best in both low visibility circumstances (0.6, and 0.3 km). One can witness that the performance disparity between HUR and other relay-assisted counterparts FOR and FHR widens as the visibility diminishes. Because FSO links have a fixed distance $L_{FSO} = \frac{L}{3}$ in counterpart models, the attenuation increases considerably if the total distance L is increased during low visibility. As expected, the single FSO link is in complete outage for both low visibility conditions.

V. Application using practical measurements

Fig. 6 plots the histogram of hourly visibility for Edinburgh and London as reported by the Meteorological Office United Kingdom for January 2019 to June 2020, totally H_{tot} = 13,106 hours (Edinburgh), H_{tot} = 13,128 hours (London). As can

$$\frac{\partial f(\chi)}{\partial \chi} = \frac{W_1}{2W_2}\left[\left(\frac{162\Omega_1\kappa \exp^{-\frac{2}{3}\kappa(L-3\chi)}}{(L-3\chi)^4} + \frac{972\Omega_1 \exp^{-\frac{2}{3}\kappa(L-3\chi)}}{(L-3\chi)^5}\right)\left(\frac{81\Omega_1 \exp^{-\frac{2}{3}\kappa(L-3\chi)}}{(L-3\chi)^4} + 1\right)^{\frac{W_1}{2W_2}-1}\right] + \frac{243\Omega_2}{(L+3\chi)^4}, \tag{19}$$

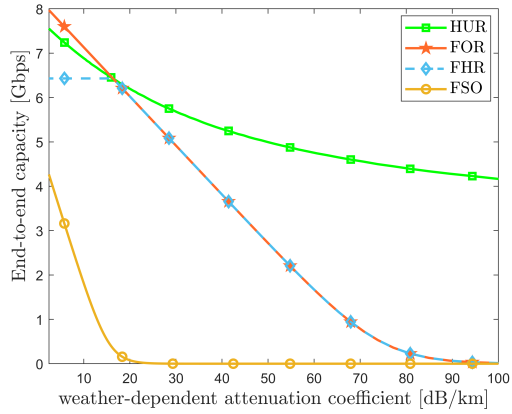

Fig. 3. End-to-end capacity $C_{\mathcal{SD}}$ versus weather attenuation coefficient κ.

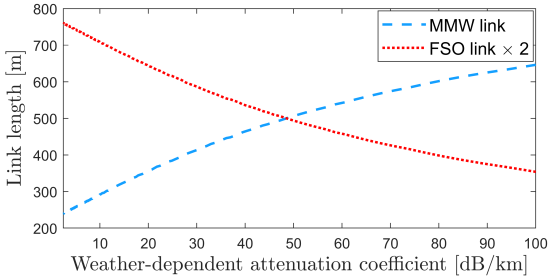

Fig. 4. Link coverage for the two FSO and one MMW hops between $\mathcal{S}$ and $\mathcal{D}$ under the proposed scheme.

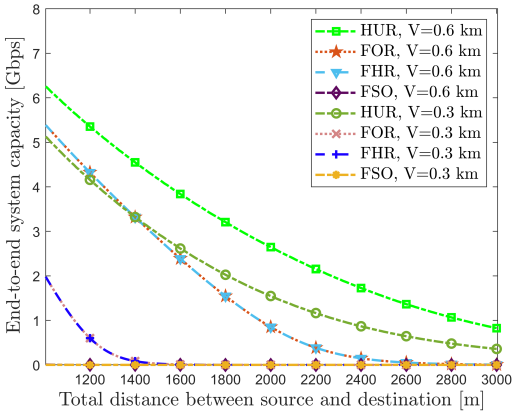

Fig. 5. End-to-end capacity of four systems versus link distance L between $\mathcal{S}$ and $\mathcal{D}$ under two poor visibility conditions.

be seen, the probability of fog events (visibility $<$ 1 km) which can severely deteriorate the FSO link's performance is significantly small. Because FSO links function well most of the time, fixed hybrid FSO/RF links with permanent or backup RF links are not necessarily the most cost-effective and practical solution all the time. To this end, short-term solutions such as the one proposed here might play a significant role in B5G networks. We use fog events to simulate the systems' capacity using the hourly visibility data with H_{fog} hours 87 and 56 for Edinburgh and London, respectively. Fig. 7

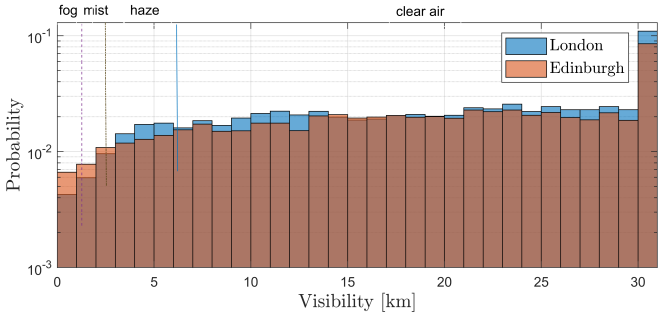

Fig. 6. Hourly visibility histogram for Edinburgh and London from January 2019 to June 2020.

demonstrates that the proposed HUR outperforms the other systems, including the FSO-only, FOR, and FHR system during the fog events in Edinburgh and London. When visibility is near to 1 km, the FOR and FHR systems rarely perform comparably to the proposed scheme. On the other hand, the HUR system performs well throughout the fog events in both London and Edinburgh, even when the counterpart models perform poorly. For example, during fog hour 13 and 40 in Edinburgh and London, respectively, the single FSO link is completely down with very minimal performance from the FOR and FHR schemes, yet the HUR still offers about 4.3 Gbps and 3.8 Gbps in Edinburgh and London, respectively.

It's also worth comparing the proposed system's link availability to FSO-only and other three-hop counterparts. The percentage of time that an atmospheric loss does not result in an outage is defined as availability, it is typically evaluated over a year or more [23]. If a specific data rate is required, the availability of a single FSO link is stated by $\mathcal{A}_{FSO} = (\mathsf{H}_{tot} - \mathsf{H}_{out})/\mathsf{H}_{tot}$, where H_{tot} is the total number of hours evaluated and H_{out} denotes the number of outage hours during which the specified data rate is not met. When the proposed system (and other three-hop) is used, however, the link availability $\mathcal{A}_{\mathrm{L}}$ may be stated as [11]

$$\mathcal{A}_{\mathrm{L}} = \frac{\sum_{k=1}^{\mathsf{H}_{\mathrm{out}}} \Theta_k^{\mathrm{ava}} + (\mathsf{H}_{\mathrm{tot}} - \mathsf{H}_{\mathrm{out}}) \times 1}{\mathsf{H}_{\mathrm{tot}}}, \tag{20}$$

where Θ_k^{ava} is the proposed system's availability probability during the kth outage hour of the FSO-only system. Assuming a minimum data rate requirement of 1 Gbps, the availability of an FSO-only link in Edinburgh and London is 99.41% and 99.6 %, respectively. The proposed HUR scheme shows 100% availability for both cities at 1 Gbps while the FOR and FHR deployments perform at 99.85% and 99.83% for Edinburgh and London, respectively. At 4 Gbps an FSO-only link is 99.34 percent available in Edinburgh and 99.57 percent in London. The proposed system offers 99.89% and 99.88% availability for Edinburgh and London, respectively. While the FOR and FHR models in Edinburgh and London respectively perform at 99.69 and 99.74 percent. The proposed scheme clearly outperforms its counterparts by achieving carrier-class availability at 1 Gbps and also exhibits superior performance than benchmark schemes at higher minimum rate requirements.

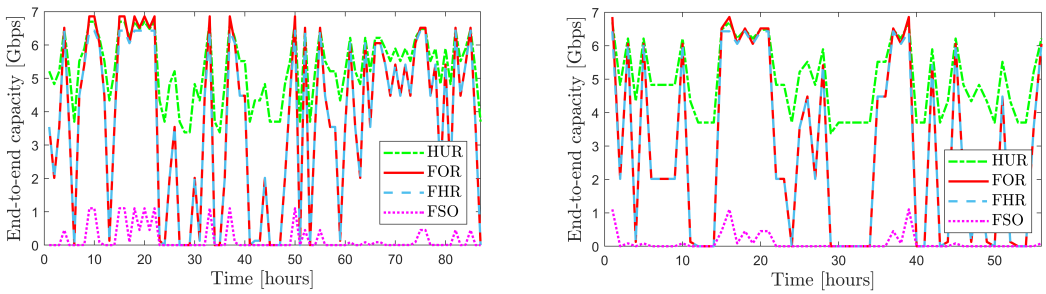

(a) Edinburgh (b) London

Fig. 7. The end-to-end capacity versus the fog hours in Edinburgh and London from January 2019 to June 2020.

VI. Conclusion

In this paper we proposed a UAV relay assisted model to improve the FSO link's capacity during the adverse weather conditions. The proposed HUR model is shown to enhance the capacity of the FSO link without making any changes at the source and destination FSO nodes. The performance of the model is compared with the benchmark single FSO, relay-assisted FSO and hybrid FSO/RF systems, proposed scheme clearly shown superior performance. The proposed system's enhanced capacity and availability over benchmark schemes is demonstrated in a realistic channel based on Edinburgh and London weather statistics. As a future work, practical challenges like UAV stability and PAT problems can be addressed when including UAVs into such highly directional deployments. The impact of non-LOS channels on UAV positioning can also be an interesting direction to pursue.

VII. Acknowledgment

The authors are grateful to the Meteorological Office of the United Kingdom for supplying measured hourly visibility data for January 2019 to June 2020 from the Edinburgh Gogarbank and the London Heathrow weather stations.

References

[1] E. T. Michailidis, P. S. Bithas, N. Nomikos, D. Vouyioukas, and A. G. Kanatas, "Outage probability analysis in multi-user FSO/RF and UAV-enabled MIMO communication networks," *Physical Commun.*, vol. 49, p. 101475, 2021.

[2] M. A. Esmail, H. Fathallah, and M. S. Alouini, "Outdoor FSO communications under fog: Attenuation modeling and performance evaluation," *IEEE Photonics Journal*, vol. 8, no. 4, pp. 1–22, 2016.

[3] M. Usman, H.-C. Yang, and M. S. Alouini, "Practical switching-based hybrid FSO/RF transmission and its performance analysis," *IEEE Photonics Journal*, vol. 6, no. 5, pp. 1–13, 2014.

[4] S. Bloom and W. S. Hartley, "The last-mile solution: hybrid FSO radio," *Whitepaper, AirFiber Inc*, pp. 1–20, 2002.

[5] A. Engelmann and A. Jukan, "Serial, parallel or hybrid: Towards a highly reliable transmission in RF/FSO network systems," in *2015 IEEE International Conference on Commun. (ICC)*, pp. 6181–6186, 2015.

[6] B. Zhu, J. Cheng, M. S. Alouini, and L. Wu, "Relay placement for FSO multihop DF systems with link obstacles and infeasible regions," *IEEE Trans. on Wireless Commun.*, vol. 14, no. 9, pp. 5240–5250, 2015.

[7] N. Tafintsev, D. Moltchanov, M. Gerasimenko, M. Gapeyenko, J. Zhu, S.-p. Yeh, N. Himayat, S. Andreev, Y. Koucheryavy, and M. Valkama, "Aerial access and backhaul in mmwave B5G systems: Performance dynamics and optimization," *IEEE Commun. Magazine*, vol. 58, no. 2, pp. 93–99, 2020.

[8] T. Hou, Y. Liu, Z. Song, X. Sun, and Y. Chen, "UAV-to-everything (U2X) networks relying on NOMA: A stochastic geometry model," *IEEE Trans. on Vehicular Tech.*, vol. 69, no. 7, pp. 7558–7568, 2020.

[9] E. Erdogan, I. Altunbas, N. Kabaoglu, and H. Yanikomeroglu, "A cognitive radio enabled RF/FSO communication model for aerial relay networks: Possible configurations and opportunities," *IEEE Open Journal of Vehicular Tech.*, vol. 2, pp. 45–53, 2021.

[10] G. Castellanos, M. Deruyck, L. Martens, and W. Joseph, "Performance evaluation of direct-link backhaul for UAV-aided emergency networks," *Sensors*, vol. 19, no. 15, p. 3342, 2019.

[11] S. Huang, V. Shah-Mansouri, and M. Safari, "Game-theoretic spectrum trading in RF relay-assisted free-space optical communications," *IEEE Trans. on Wireless Commun.*, vol. 18, no. 10, pp. 4803–4815, 2019.

[12] G. Farhadi and N. Beaulieu, "On the ergodic capacity of multi-hop wireless relaying systems," *IEEE Trans. on Wireless Commun.*, vol. 8, no. 5, pp. 2286–2291, 2009.

[13] J.-H. Lee, K.-H. Park, Y.-C. Ko, and M. S. Alouini, "Throughput maximization of mixed FSO/RF UAV-aided mobile relaying with a buffer," *IEEE Trans. on Wireless Commun.*, vol. 20, no. 1, pp. 683–694, 2021.

[14] A. A. Farid and S. Hranilovic, "Outage capacity optimization for free-space optical links with pointing errors," *Journal of Lightwave Tech.*, vol. 25, no. 7, pp. 1702–1710, 2007.

[15] V. Jamali, D. S. Michalopoulos, M. Uysal, and R. Schober, "Link allocation for multiuser systems with hybrid RF/FSO backhaul: Delay-limited and delay-tolerant designs," *IEEE Trans. on Wireless Commun.*, vol. 15, no. 5, pp. 3281–3295, 2016.

[16] H. E. Nistazakis, T. A. Tsiftsis, and G. S. Tombras, "Performance analysis of free-space optical communication systems over atmospheric turbulence channels," *IET Commun.*, vol. 3, no. 8, pp. 1402–1409, 2009.

[17] T. S. Rappaport, S. Sun, R. Mayzus, H. Zhao, Y. Azar, K. Wang, G. N. Wong, J. K. Schulz, M. Samimi, and F. Gutierrez, "Millimeter wave mobile communications for 5G cellular: It will work!," *IEEE Access*, vol. 1, pp. 335–349, 2013.

[18] S. Sharma, A. S. Madhukumar, and R. Swaminathan, "Switching-based cooperative decode-and-forward relaying for hybrid FSO/RF networks," *Journal of Optical Commun. and Networking*, vol. 11, no. 6, pp. 267–281, 2019.

[19] F. Nadeem, V. Kvicera, M. S. Awan, E. Leitgeb, S. S. Muhammad, and G. Kandus, "Weather effects on hybrid FSO/RF communication link," *IEEE Journal on Selected Areas in Commun.*, vol. 27, no. 9, pp. 1687–1697, 2009.

[20] B. He and R. Schober, "Bit-interleaved coded modulation for hybrid RF/FSO systems," *IEEE Trans. on Commun.*, vol. 57, no. 12, pp. 3753–3763, 2009.

[21] F. Fontana and E. Bozzo, "Newton–raphson solution of nonlinear delay-free loop filter networks," *IEEE/ACM Trans. on Audio, Speech, and Language Processing*, vol. 27, no. 10, pp. 1590–1600, 2019.

[22] M. A. Esmail, H. Fathallah, and M.-S. Alouini, "On the performance of optical wireless links over random foggy channels," *IEEE Access*, vol. 5, pp. 2894–2903, 2017.

[23] I. I. Kim, R. Stieger, J. Koontz, C. Moursund, M. Barclay, P. Adhikari, J. J. Schuster, E. J. Korevaar, R. Ruigrok, and C. M. DeCusatis, "Wireless optical transmission of fast ethernet, FDDI, ATM, and ESCON protocol data using the terralink laser communication system," *Optical Engineering*, vol. 37, no. 12, pp. 3143–3155, 1998.